

Fiber Tractography in Diffusion Tensor Magnetic Resonance Imaging: A Survey and Beyond

Jun Zhang*, Hao Ji, Ning Kang, Ning Cao
Laboratory for High Performance Scientific Computing and Computer Simulation,
Department of Computer Science, University of Kentucky,
Lexington, KY 40506-0046, USA

April 11, 2005

Abstract

Diffusion tensor magnetic resonance imaging (DT-MRI) is the first noninvasive *in vivo* imaging modality with the potential to generate fiber tract trajectories in soft fibrous tissues, such as the brain white matter. Several newly developed fiber reconstruction and tractography techniques based on DT-MRI are reviewed in this article, including streamline fiber tracking techniques, diffusion tensor deflection strategy, probabilistic Monte-Carlo method, fast marching tractography based on level set principles, and diffusion simulation-based tractography. We also discuss some potential applications of DT-MRI fiber tractography and list a few available tractography and visualization software packages.

Key words: Diffusion tensor magnetic resonance imaging, fiber tractography, streamline tracking, anisotropic diffusion simulation

1. Introduction to DT-MRI

The complexity of the human brain presents tremendous challenges in *in vivo* understanding its inter-structure and functionality. The nature of the human brain imposes substantial difficulty in noninvasive studies in which magnetic resonance imaging (MRI) plays an important role. Diffusion tensor magnetic resonance imaging, or DT-MRI [5,7,37], is an extension of the conventional MRI with the added capability of tracking and measuring the random motion of water molecules in all three dimensions, usually referred to as self-diffusion or “Brownian motion”. Since water diffusion is influenced by the microstructure, architecture, and physical properties of tissues, DT-MRI can render the information about how water diffuses in biological tissues containing a large number of fibers, like muscles or brain white matter, into intricate three

* Technical Report No. 437-05, Department of Computer Science, University of Kentucky, Lexington, KY, 2005. The research work of this author was supported in part by the U.S. National Science Foundation under grants CCR-0092532 and ACR-0202934, and in part by the U.S. Department of Energy Office of Science under grant DE-FG02-02ER45961. E-mail: jzhang@cs.uky.edu, URL: <http://www.cs.uky.edu/~jzhang>.

dimensional (3D) representations of tissue architecture. Thus, it can be exploited to visualize and extract information about the brain white matter and nerve fibers by probing and reconstructing the fiber pathways, which has raised promises for achieving a better comprehension of the fiber tract anatomy of the human brain [10]. In fact, one of the aims of using DT-MRI is the *in vivo* reconstruction of neural connectivity and the determination of fiber networks in the brain. In combination with functional MRI (fMRI), it might potentially bring tremendous improvements in our understanding of the crucial issue of anatomical connectivity and functional coupling between different regions of the brain [14,21,33,38]. As a result, the brain tissue diffusion properties and the neuro-anatomical knowledge on connectivity interpreted from the DT-MRI information have been playing an indispensable role in neurosurgery planning [15,71] and in tackling certain brain diseases and disorders, such as Alzheimer's disease [58,63], stroke [26], multiple sclerosis [17,66], schizophrenia [3,18], etc.

It is known that water diffusion is anisotropic in brain white matter. The significant anisotropy presenting in white matter reveals microscopic properties of the anatomy of the nerve fibers by the fact that water tends to diffuse predominantly along the long axis of the fibers, because the longitudinally oriented structures, the densely packed axons and the inherent axonal membranes, which are widely assumed to be the main barrier for water diffusion, hinder diffusion perpendicular to the fibers [10]. DT-MRI is sensitive to this anisotropy and is able to characterize it by noninvasively quantifying and assessing the self-diffusion of water *in vivo*. The information concerning the local orientation of fibers, extracted from the water anisotropic diffusion in white matter, forms the basis of utilizing DT-MRI to reconstruct fiber pathways and to build connectivity map *in vivo*. The water diffusion behavior elucidated by DT-MRI reflects the directional organization of the underlying white matter microstructure. DT-MRI characterizes the diffusion behavior on a voxel by voxel basis and for each voxel, the diffusion tensor yields the diffusion coefficient corresponding to any direction in space [5]. The direction of the greatest diffusion can be determined by evaluating the diffusion tensor in each voxel, which corresponds to the dominant axis of the white matter fiber bundles traversing the voxel.

The diffusion tensor at each voxel is a three-by-three symmetric (semi-positive definite) matrix [5],

$$D = \begin{pmatrix} D_{xx} & D_{xy} & D_{xz} \\ D_{yx} & D_{yy} & D_{yz} \\ D_{zx} & D_{zy} & D_{zz} \end{pmatrix},$$

which geometrically can be visualized as a 3D ellipsoid [74]. The three eigenvalues $\lambda_1 \geq \lambda_2 \geq \lambda_3 \geq 0$ and the associated eigenvectors e_1, e_2 and e_3 of D fully define the ellipsoid. The three eigenvectors are the three orthogonal axes of the ellipsoid, whose lengths are the magnitudes of the three eigenvalues. The eigenvalues and eigenvectors of D provide rich information about local orientation of the tissue structures.

To provide an intuition for the tensor data, derived from the measured diffusion-weighted and diffusion-unweighted images, an axial slice of a diffusion tensor volume from the human brain is depicted in Fig. 1. It shows a matrix of images, where each image is a color-coded representation of the corresponding component of the tensor matrix D .

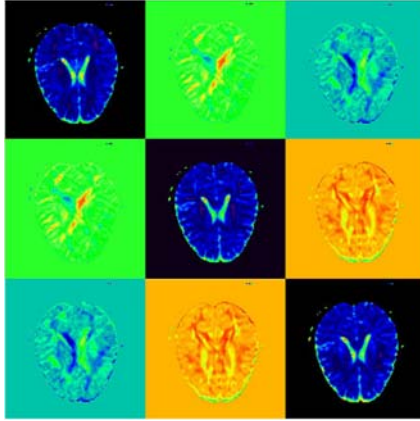


Figure 1: An axial slice of a diffusion tensor data volume, which shows the individual diffusion tensor components, corresponding to the diffusion tensor matrix D .

Some of the most frequently used diffusion anisotropy parameters in DT-MRI studies are defined based on the eigenvalues of D . For example, the fractional anisotropy (FA) value is defined as [7]

$$FA = \sqrt{\frac{3}{2}} \sqrt{\frac{(\lambda_1 - \bar{D})^2 + (\lambda_2 - \bar{D})^2 + (\lambda_3 - \bar{D})^2}{\lambda_1^2 + \lambda_2^2 + \lambda_3^2}},$$

where $\bar{D} = \frac{1}{3} \text{Trace}(D) = \frac{1}{3}(\lambda_1 + \lambda_2 + \lambda_3)$. The FA value is 0 for diffusion in purely isotropic medium and 1 for diffusion in strongly anisotropic medium. Other parameters characterizing diffusion anisotropy, such as the mean diffusivity, lattice index, and intervoxel coherence, are also computed and compared in a few studies [55,56,58,77,78]. For excellent review articles on general aspects of diffusion tensor imaging, we refer to [4,38,39]. For more specific application-oriented reviews on diffusion tensor imaging, interested authors should consult [15,34,46,64].

The information in the DT-MRI data can be exploited to reconstruct the fiber pathways of the brain. A number of fiber tracking algorithms, or tractography, have been developed since the advent of DT-MRI [6,11,14,20,29,44,54,52]. In the following sections we will examine a few different fiber tracking techniques, explain their advantages, limitations, and potential applications, followed by a list of some available fiber tractography and visualization software packages. This survey focuses on accounting for the algorithmic difference of the various fiber tracking techniques, with an emphasis on diffusion simulation-based tractography. For recent reviews focusing on basic principles and assumptions and reliability analysis of fiber tractography, with an emphasis on streamline-based tractography, we refer to [42,45].

2. Streamline Fiber Tracking

The conventional white matter tractography reconstructs the pathways of white matter tracts by starting from a seed voxel and tracing down the trajectory in a voxel-by-voxel manner, using an estimate of the local fiber orientation determined by the principal eigenvector in each voxel. At

each voxel, the principal eigenvector, which is the one corresponding to the largest eigenvalue generated by the eigen decomposition of the diffusion tensor, is aligned with the mean fiber direction in that voxel. Hence, trajectories can be produced by integrating the principal eigenvector field, which are expected to coincide with white matter fiber bundles. Efforts have been made to trace the neural fiber pathways in white matter tracts by this method and its variants [6,14,44,62,76,79] and very impressive results on major fiber structures have been demonstrated. The approaches to fiber reconstruction based on this idea are sometimes referred to as streamline tracking techniques [36,54], stemming from their similarity to computing flow streamlines from the velocity fields in fluid dynamics.

The most popular streamline tracking algorithm, proposed by Basser *et al.* [6], uses the direction of the eigenvector e_1 associated with the largest eigenvalues λ_1 as the direction of the local fiber orientation. Given an initial seed tracking point $s(0)$, we can solve a 3D path equation [6]

$$\frac{ds(t)}{dt} = r(t), \quad (1)$$

where $s(t)$ is the fiber curve path position at t and $r(t)$ is the local tangent direction of the path $s(t)$. We can set $r(t) = \varepsilon e_1(t)$ with $e_1(t)$ being the eigenvector e_1 at t and ε being a small positive number.

Eq. (1) can be solved numerically by either the Euler's method or some high order Runge-Kutta method. The integrated path is connected as the path of one fiber tract. A fiber bundle can be reconstructed by slightly perturbing the initial seed point and by generating multiple tracts following the same orientation and from the same region of interest (ROI).

In practice, care must be exercised to ensure that the DT-MRI data are properly collected and pre-processed. Since the resolution of most MRI data is usually not as good as the tracking algorithms prefer to have, mathematical techniques can be used to pre-process the DT-MRI data. Pajevic *et al.* [50] proposed to generate a continuous DT-MRI data field using interpolation, which allows integration step size to be smaller than the voxel size. Since the directions of both e_1 and $-e_1$ are valid, tracks may be followed in both directions at the seed point (and along the forward path direction at the subsequent points) until certain termination conditions are met. Those termination conditions are set based on our understanding of the properties of the fiber tracts.

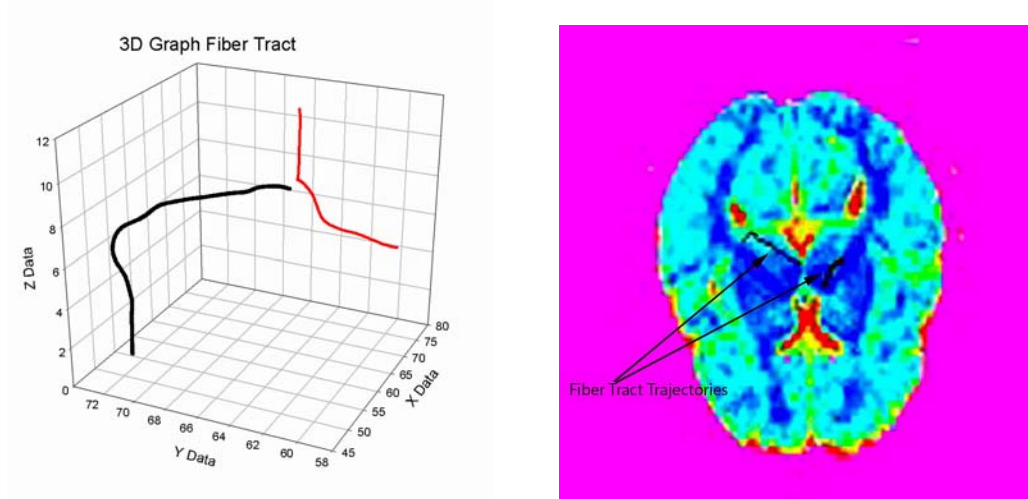


Figure 2: Two fiber tracts traced using a streamline-based tracking method in a healthy human brain (left panel) and their projection on an MR image (right panel).

The streamline fiber tracking algorithms, based on the ideas proposed by Basser *et al.* [6], have been implemented by a few groups. Fig. 2 shows two traced fiber tracts and their projection on a DT-MR image, produced in our lab using the streamline tractography.

The streamline-based tracking technique is the one most commonly used in white matter tractography studies and it appears to give excellent results in many instances if the principal eigenvector field is smooth and the fibers are strongly oriented along a certain direction. It is easy to implement and runs fast to trace individual fiber tracts. However, this technique suffers from a few major limitations. As noticed and summarized in [36,57], the vector field is error prone in the sense that the noise of DT-MRI data will influence the direction of the principal eigenvector, yielding an accumulation of orientational errors and thus an erroneous fork of the trajectory reconstruction process. Another major restriction is that it may also be affected by partial volume effects [75], leading to an unstable tracking of fibers through the primary eigenvector field. Since the current resolution of DT-MRI is 1-4 *mm* while the diameter of the nerve fibers is in the magnitude of μm , in regions of fiber crossing, branching, or merging, the measured diffusion tensor data is difficult to interpret, which represents a complicated averaging of multiple compartments within a voxel, making the principal eigenvector field not adequate to describe such entangled structures.

3. Diffusion Tensor Deflection

A variety of methods have been proposed aiming to overcome the difficulties to which the streamline tracking technique is exposed, with more information incorporated from the diffusion tensor data. In recent years, stochastic labeling method [65], bootstrap analysis [22], multi-ROI approach [23], and others have been proposed to enhance and assess DT-MRI fiber tracking. One improved approach to determining tract direction was proposed by Lazar *et al.* [36,73] using the entire diffusion tensor to deflect the incoming vector v_{in} direction:

$$v_{out} = D \cdot v_{in} \quad (2)$$

The incoming vector represents the propagation direction from the previous integration step. The tensor operator deflects the incoming vector towards the major eigenvector direction, but limits the curvature of the deflection, which should result in smoother tract reconstructions. The algorithm is called TEND for tensor deflection.

In the TEND algorithm, the incoming vector, v_{in} , can be conveniently described by using a linear combination of the three diffusion tensor eigenvectors:

$$v_{in} = \alpha_1 e_1 + \alpha_2 e_2 + \alpha_3 e_3 \quad (3)$$

where α_1 , α_2 and α_3 are the relative vector weightings. By multiplying both sides of Eq. (3) with D , substituting $\lambda_i e_i$ for $D \cdot e_i$ (the characteristic matrix equation), and normalizing to the largest eigenvalue, Eq. (2) can be rewritten as:

$$v_{out} = \lambda_1 \left(\alpha_1 e_1 + \frac{\lambda_2}{\lambda_1} \alpha_2 e_2 + \frac{\lambda_3}{\lambda_1} \alpha_3 e_3 \right)$$

where v_{out} is an unscaled vector, e_1 , e_2 , and e_3 are unit vectors. Several specific cases can be treated separately. If the incoming vector coincides with one of the tensor eigenvectors, all α 's will be zero except the one corresponding to the eigenvector direction and v_{in} will not be deviated by the tensor (i.e., $v_{out} = v_{in}$). The degree of tensor deflection can be a function of the diffusion tensor anisotropy and the angle between v_{in} and e_1 .

For a highly prolated diffusion tensor (e.g., $\lambda_1 \gg \lambda_2, \lambda_3$), and α_1 not much less than α_2 or α_3 , the output vector of the TEND algorithm will be deflected towards the direction of the major eigenvector, $v_{out} = \lambda_1 \alpha_1 e_1 + \Delta \approx \lambda_1 \alpha_1 e_1$. However, for $\alpha_1 \gg \alpha_2$ or α_3 , the tract direction will not be highly deflected.

For an oblate shaped diffusion tensor (e.g., $\lambda_1 \approx \lambda_2 \gg \lambda_3$) and α_3 small, the deflected vector is $v_{out} = \lambda_1 (\alpha_1 e_1 + \alpha_2 e_2)$. In this case, both the major and medium eigenvectors affect the deflection. The incoming vector component perpendicular to the tensor plane (defined by e_3) will be adjusted so that the incoming vector will be deflected toward the ellipsoid plane. This behavior may be desirable for voxels with planar diffusion where eigenvector degeneracy can occur and the direction of the fastest diffusivity is not well defined. The planar tensor shape may

appear in regions with crossing, fanning, or merging fibers [1,75]. However, where v_{in} is roughly in the e_3 direction, the incoming vector will be relatively undeflected.

For an isotropic tensor (e.g., $\lambda_1 \approx \lambda_2 \approx \lambda_3$), the incoming vector will not be significantly deviated, $v_{out} \approx \lambda_1(\alpha_1 e_1 + \alpha_2 e_2 + \alpha_3 e_3) \equiv v_{in}$.

The tracking results reported in [36] show that the diffusion tensor deflection method is less sensitive to both image noise and lower tensor anisotropy. In general, the TEND algorithm will be able to trace longer fiber trajectories than the standard streamline-based tracking techniques do. However, tensor deflection method will underestimate the trajectory curvature for curved pathways [36]. This error is cumulative, but can be reduced by using smaller step sizes. Consequently, there is a tradeoff between lower error with the tensor deflection algorithm in straighter sections, but higher systematic errors in curved sections. One approach to balancing this tradeoff is to use a combined streamline tracking and tensor deflection algorithm. The tensorline algorithm, proposed by Weinstein *et al.* [73], dynamically adjusts a hybrid of the streamline and TEND algorithms in the form of

$$v_{out} = f e_1 + (1-f)[(1-g)v_{in} + gD \cdot v_{in}],$$

in which f and g are some user-defined weighting parameters that are between 0 and 1. Due to the flexibility in adjusting the parameters f and g , it is possible for the tensorline algorithm to map trajectories with different properties. The tensorline algorithm may be considered as a family of tractography algorithms that can be “tuned” to accommodate specific fiber tract behaviors [36]. The drawback, of course, is the need to handle these user-defined parameters, which makes the algorithm less automatic.

4. Probabilistic Monte-Carlo Method Based Tracking

Parker *et al.* [51,52] proposed a probabilistic Monte-Carlo method to decide the mapping of brain connections for quantifying streamline-based diffusion fiber tracking methods. In this approach, the traditional streamline method is used to exploit the uncertainty in orientation of the principal direction of diffusion defined for each image voxel. By repeatedly running the streamline process the Monte-Carlo methods exploit the inherent uncertainty in the DT-MRI data to generate maps of connection probability. Uncertainty is defined by interpreting the shape of the diffusion orientation profile provided by the diffusion tensor in terms of the underlying microstructure [52].

Recall the introduction to streamline tracking algorithm in the earlier section, $r(t)$ in Eq. (1) is the local tangent direction of the path $s(t)$. It can be set to $\mathcal{E}_1(t)$ with $e_1(t)$ being the

eigenvector e_1 at t and ε being a small positive number. To define an anatomically reasonable interpretation of the diffusion tensor for probabilistic connectivity analyses, the probabilistic method exploits the uncertainty of the e_1 orientation (principal eigenvector orientation) in the connectivity analysis. A general framework was proposed in [52] that allows the use of any probability distribution functions (PDFs) describing the fiber orientation distribution. Two candidate PDFs are defined as the $0th$ order and the $1st$ order to reflect their complexity. In the $0th$ order case, uncertainty in the e_1 is defined by tensor anisotropy, providing an isotropic normal distribution of orientation centered on the original estimate of e_1 . In the $1st$ order case, the orientations of the minor eigenvectors e_2 and e_3 , and their respective eigenvalues provide an uncertainty that is dependent upon the skewness of the tensor, thus providing a more accurate distribution of the orientation in the case of oblate tensor ellipsoids. Streamline propagation is then repeated in a Monte-Carlo process using the PDFs, thus establishing the confidence of connection to the starting point to a distributed area, from a fundamentally linear process.

Besides the choices of PDFs in [52], a number of alternative PDFs can also be chosen for the determination of a probabilistic index of connectivity. The experimental results in [51,52] show that this improved tracking method could somehow reveal more inherent voxel fiber tract topology and hopefully can improve the tracking result under the situation of fiber crossing and diverging.

5. Level Set-Based Fast Marching Tractography

A new algorithmic development trend in DT-MRI tractography is to make use of the front propagation algorithms [53,67]. Front propagation-based tractography methods have two advantages over the streamline-based methods. First, front propagation algorithms are capable of estimating branching and crossing tract structures in a more straightforward and computationally efficient manner than modified streamline techniques. Second, unlike streamline tracking, front propagation algorithms may estimate the likelihood of white matter connectivity between any two voxels.

Recently, level set theory, which models the evolution of a front over time, is utilized to find the fiber paths connecting different brain regions. Parker *et al.* [53, 54] proposed a fast marching tractography method (FMT). FMT is based on the level set theory and a fast marching algorithm [60] in which a front interface propagates in directions normal to itself with a non-negative speed function. A time of arrival map is created for every point in a gridded space by recording the time at which the front passes each grid point. The relationship between the time, T , and the speed, F , during the front propagation, is given by the Eikonal equation [61] $|\nabla T|F = 1$. The FMT algorithm begins at the seed point with the consideration of the nearest neighbors around the seed

point. In the 3D case, the 6 nearest neighbors are defined as being in the Up, Down, North, South, East and West directions. A potential time of front arrival is assigned to each of the neighboring candidate points (voxels) using the following equation

$$T(r) = T(r') + \frac{|r - r'|}{F(r)},$$

where r is a position vector specifying the grid location of a candidate point. The position vector r' describes the grid location of the closest point to r along the normal direction to the front, $-\hat{n}(r)$, that has already been passed by the front. The normal to the front may be calculated with 26 neighbor connectivity in 3D using Eqs. (4) - (6).

$$\hat{n}(r) = \frac{\nabla f(r)}{|\nabla f(r)|} \quad (4)$$

$$\nabla f_x(r) \approx \sum_{i=-1}^1 \sum_{j=-1}^1 \sum_{k=-1}^1 C_i(r_x - i, r_y - j, r_z - k) \quad (5)$$

$$C_{i,j,k}(r_x - i, r_y - j, r_z - k) = \begin{cases} i, j, k & : (r_x - i, r_y - j, r_z - k) \in S(p) \\ 0 & : (r_x - i, r_y - j, r_z - k) \notin S(p) \end{cases} \quad (6)$$

In Eq. (4), $\nabla f(r)$ is a concentration gradient of past band points that have already been passed by the front, f , as seen from a local candidate band position r . The concentration gradient $\nabla f(r)$ is a vector composed of three Cartesian components: $\nabla f_x(r)$, $\nabla f_y(r)$, and $\nabla f_z(r)$. Eq. (6) discretely approximates $\nabla f(r)$ using the concentration differences in the set of past band positions, $S(p)$, that have already passed by the front.

The seed point is considered to have already been passed by the front before the first iteration of the front propagation tractography algorithm. The speed function $F(r)$ determines the speed of the propagation from r' to a candidate position r . The candidate point with the fastest time of arrival, $T(r)$, is selected as the next point of front arrival. The newest point is assigned a fixed time of arrival value $T(r)$, and a fixed speed of arrival value $F(r)$. The newest point of arrival at r is removed from the candidate band and is never considered again during the propagation. The propagation continues as new times of arrival are calculated from points within the 6 point neighborhood of r that have yet to be reached by the front. Times of arrival for unselected candidate points are modified if the time of arrival for the current iteration is less than the time of the previous iterations. The propagation continues until every point on the grid is assigned a time of arrival value.

The FMT algorithm uses the orientation and shape of the diffusion tensor D to define the speed function F . The premise of FMT is that the front propagation speed is controlled by using D such that the front propagates fastest within white matter tracts. An example of an FMT speed function developed by Parker *et al.* [54] is

$$F(r) = \min(F(r'), |\hat{v}_1(r') \cdot \hat{n}(r)|),$$

where the term $F(r')$ refers to the overall minimum historical speed of propagation to the point of the current iteration. The quantity $|\hat{v}_1(r') \cdot \hat{n}(r)|$ is the absolute value of the scalar product between the principal eigenvector at the latest point accepted into the past band and the unit normal vector to the front from a candidate point at position r . The term $|\hat{v}_1(r') \cdot \hat{n}(r)|$ causes the front to propagate fastest in the direction of the principal eigenvector field. The historical minimum speed is used to establish connectivity between the starting point and all successive points of the propagation. Thus, the FMT algorithm does use the principal eigenvector information to define the speed and direction of the propagation.

In FMT, the time of arrival map from the seed point to other points in the DT-MRI volume is used to construct minimum cost paths between the seed point and other points on the grid. Because diffusion tensor orientation is embedded in the time of arrival map, maximum speed paths from an end point to the seed point in a DT-MRI volume are estimates of white matter tract connectivity between the two points. Diverging tract structures may be inferred using FMT by constructing maximum speed tracts to the seed point using each point on the grid as a potential tract end point. In the process of traversing maximum speed tracts back to the seed point, some tracts will converge or cross, indicating the presence of crossing and diverging structure.

The likelihood metric capability of FMT allows for confidence estimates of white matter connectivity between any two points in a volume of DT-MRI data. An example of an FMT likelihood function can be $L(\gamma) = \min(F(\gamma(s)))$ where $\gamma(s)$ is a minimum cost tract between an end point and the seed point parameterized by s . Because the front propagates fastest inside regions of homogeneous diffusion tensor orientation, higher speeds over the extent of a tract indicate that a putative tract is more likely to be a legitimate anatomical structure than an artifact.

Level set theory has also been used in [13,25] to implement a 3D geometrical flow to track the fiber bundles. The major disadvantage of this class of tractography is the difficulty to determine the true fiber trajectories from the possibly multiple constructed trajectories and the need to use the principal eigenvector direction to advance the fronts.

6. Diffusion Simulation-Based Fiber Tractography

As the measured quantity in DT-MRI is for water diffusion, an intuitive way to gain insights from the diffusion tensor data is to carry out a *direct* simulation of water diffusion, which is anisotropic and governed by the diffusion equation, over the brain. The idea of studying brain connectivity by

simulating the anisotropic diffusion has been preliminarily explored in [9,20,48], and [8] further extends the diffusion equation to a diffusion-convection equation by adding a convection term. However, in the above mentioned work based on this insight, there is no (or at best limited) attempt at determining the route of fiber pathways and connectivity between anatomical or functional regions in the brain, although the concentration or flow field over the brain is calculated and obtained. Kang *et al.* [29,31] proposed a new technique along this line, which relies on successive anisotropic diffusion simulations over the whole brain, and is utilized to construct 3D diffusion fronts.

6.1. Anisotropic diffusion in brain

In diffusion simulation-based fiber tractography, the whole 3D brain volume is treated as an anisotropic physical system, over which a virtual water diffusion process is simulated. A thorough discussion on the diffusion process and related transport mechanisms in brain can be found in [35,47]. Anisotropic systems are those that exhibit a preferential spreading direction while isotropic systems are those that have no preference. According to Fick's macroscopic law of diffusion [16], which illustrates the physical behavior of the diffusion process, the flux, J , is related to the concentration, ρ , by the equation

$$J = -D\nabla\rho \quad (7)$$

This equation states that the concentration gradient $\nabla\rho$ causes the flux J which aims to compensate for this gradient. Substituting Eq. (7) into the continuity equation

$$\frac{\partial\rho}{\partial t} + \nabla \cdot J = 0$$

which expresses the conservation law of mass. The equation governing the general anisotropic diffusion process can be written as

$$\frac{\partial\rho}{\partial t} = \nabla \cdot (D\nabla\rho), \quad (8)$$

where t is the independent time variable. Since the brain tissue is not only anisotropic but also heterogeneous, the diffusion tensor D in such a case is space-dependent and thus the spatial derivatives of the tensor components D_{xx} , D_{xy} , D_{xz} , etc., must be utilized.

6.2. Constructing successive diffusion fronts

The fundamental idea behind the diffusion simulation-based fiber tracking algorithm (DFTA) is to perform successive diffusion simulations over the brain stemming from a series of selected starting voxels where a seed is placed. With certain thresholds satisfied, the starting voxels are dynamically picked up from the nodes on the 3D diffusion fronts produced by previous rounds of the diffusion simulation. Thus the first step to reconstruct fiber pathways starts with choosing a root node s . The virtual concentration seed of water spreads from the root node through neighboring nodes, within a limited amount of time, forming a diffusion front which is the surface

of a diffusion volume containing nodes with nonzero¹ concentration values. The expansion of the diffusion volume originated from the root voxel is achieved by integrating the anisotropic diffusion equation (8) through the whole brain over a certain amount of time, subject to the following initial condition,

$$\rho|_{t=0} = \begin{cases} 1 & \text{at the root voxel} \\ 0 & \text{otherwise} \end{cases} \quad (9)$$

For the boundary condition of Eq. (8), we assume that the physical system containing the brain is insulated, i.e.,

$$(D\nabla\rho) \cdot \bar{n} = 0 \quad (10)$$

which corresponds to the Neumann condition. Here \bar{n} is the direction normal to the brain boundary. This condition implies that the normal part of the gradient of the concentration on the boundary is zero, in other words, nothing escapes out of the computational domain. An unsteady state anisotropic diffusion solver framework has been developed and implemented which is adapted to the cerebral circumstance and runs in both sequential and parallel computing environments [27,28].

In order to construct the diffusion front propagated from a root voxel, DFTA only integrates over a fine-tuned amount of time the equation (8) through the whole brain using the developed time-dependent diffusion solver framework [27,28]. The length of the integration time is determined in such a way that without the loss of revelations of the anatomical properties of the underlying nerve fibers, the number of voxels swept by the diffusion process should be as small as possible. This value is chosen according to several factors including the magnitude of the tensor data, the spatial resolution of the computational grid, and the initial concentration at the root voxel. Once the time integration procedure is completed, a discrete approximation to the diffusion front can be calculated in terms of whether the concentration value is zero in a voxel. Thus all nodes in the computational grid can be partitioned into two groups, one with zero concentration value and the other with nonzero value. Let $V(r)$ denote the set of voxels that have nonzero concentration value, where r is the position of the root node. Since only a seed is diffused over the root node, the set $V(r)$ is comprised of the nodes in the diffusion-swept volume. For each member of $V(r)$, we consider its surrounding 6 closest neighboring nodes in a $3 \times 3 \times 3$ kernel. Let i, j, k index the relative coordinates of the 6 nearest neighbors to r with $i, j, k \in \{-1, 0, 1\}$. If $F(r)$ is the set of voxels that form the diffusion front of r , then for any node $p \equiv (p_x, p_y, p_z) \in V(r)$, we define

¹ Zero concentration values mean values close to zero. A threshold can be applied to determine zero and nonzero values.

$$p \in F(r) \text{ if and only if } \begin{cases} \exists i, & (p_x - i, p_y, p_z) \notin V(r) \text{ or} \\ \exists j, & (p_x, p_y - j, p_z) \notin V(r) \text{ or} \\ \exists k, & (p_x, p_y, p_z - k) \notin V(r) \end{cases} \quad (11)$$

Fig. 3 is an illustration of the discrete approximation to a diffusion front seed-diffused from a root voxel r .

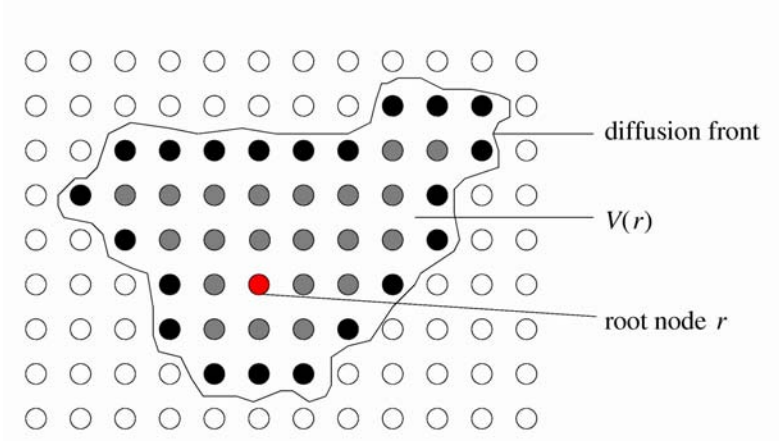


Figure 3: An illustration of the discrete approximation to a diffusion front, which borders the diffusion-swept volume $V(r)$ containing the node r (shown in red) as the root where a seed is diffused and the grey nodes with nonzero concentration value. Those originally grey nodes that satisfy condition (11) are colored black, which are used to approximate the front. The white nodes are the ones with zero concentration value.

A queue Q , a first-in first-out data structure, is set up to store and handle the dynamically produced front nodes. Q is initialized to contain just the starting node s ; thereafter, Q always contains the set of diffusion front nodes. We also define a set C to bear a number of criteria, which controls the connection of fiber pathways [29,31]. Once $F(r)$ is computed for the root node r , the algorithm further applies the criteria in C to the nodes of $F(r)$ and pick up those that meet the corresponding thresholds. Define $I(r)$ to be the set of nodes selected from $F(r)$ that satisfy the criteria in C . $I(r)$ is then appended to the tail of the queue Q . The current head node of Q is removed off the queue and is considered to be a new root r' where a seed is diffused, and its diffusion front $F(r')$ is calculated in the same way as that of $F(r)$ by solving and integrating the equation (8) over a certain amount of time through the whole brain.

The algorithm continues in this way by repeatedly taking off the head node of Q and processing it as a new root to diffuse a seed over it, until the queue becomes empty.

6.3. Fiber tracking algorithm

During the construction of successive 3D diffusion fronts, the connection between a diffusion root node r and the nodes in its diffusion front $F(r)$ may determine the possible routes of the fiber tract going through both r and $F(r)$. As mentioned earlier, the connectivity is regulated by the criteria set C , which determines the members of $I(r)$. The fiber pathways passing the node r and its diffusion front can be obtained by just connecting r and the nodes in $I(r)$. Obviously, fiber branching is allowed in this way since the size of the set $I(r)$ can be greater than 1 such that the tracking route is allowed to split at r .

Aimed at recovering the fiber pathways after the construction of diffusion fronts, each voxel p in the voxel grid owns a memory of its predecessor voxel, $\pi(p)$, where $p \in I(\pi(p))$. In the current implementation of DFTA, $\pi(p)$ is the sole predecessor of p if there is one. Thus, back propagation from the voxels on diffusion fronts by following continuously the corresponding predecessor voxels may lead to paths that merge to the starting voxel s . This merging corresponds to the procedure that can be viewed in the reverse direction as fiber tracts branch outwards from s .

6.4. Results

Kang *et al.* [29,30,31] demonstrated DFTA by exploring its ability to reproduce the well-known course of white matter structures. Fig. 4 shows the reconstructed fiber tracts stemming from two starting voxels located in the anterior and posterior portions of the corpus callosum, i.e., the genu and splenium, respectively. The tracking from the two starting voxels results in fibers traversing the genu and splenium and running toward the frontal and occipital poles of the two cerebral hemispheres, respectively. The trajectories are traced in parallel to the curvature of the genu and splenium, exhibiting an arch shape, which is consistent with the known anatomy. It is evident from Fig. 44 that DFTA allows tract branching since the generated fiber trajectories start from a single point and then end up with multiple points, forming a number of branching pathways from one single starting voxel. The corpus callosum commissural fibers reconstructed here are similar to those obtained in [6,14,36,76].

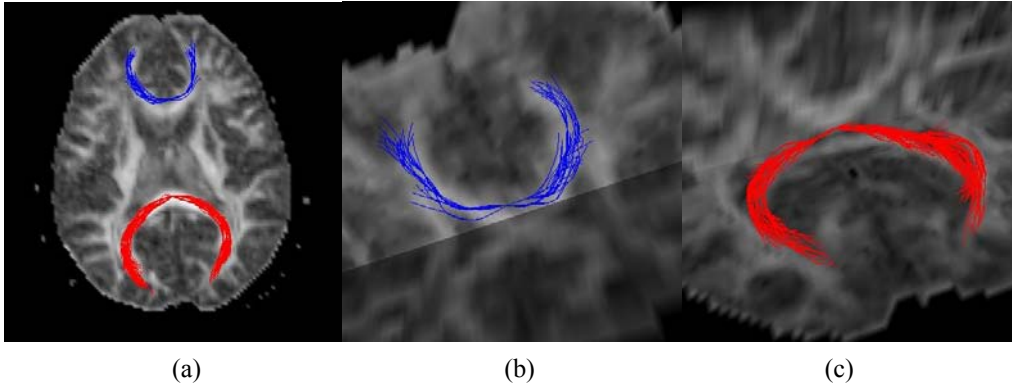


Figure 4: Fiber pathways computed from two starting voxels located in the genu and splenium of the corpus callosum (white arrow), as colored by blue and red, respectively. Fibers are incorporated into grey-scale *FA* maps for anatomical reference, where bright grey-scale regions reflect high diffusion anisotropy. (a) Fibers are viewed from the inferior direction, overlaid on an axial *FA* map. (b) and (c) Fibers are viewed from above in the anterior-left direction, shown together with a midline sagittal *FA* map as well as an axial one.

6.5. Advantages and limitations

Regarding the use of diffusion tensor data for unveiling the organizational patterns of white matter structures, the diffusion simulation-based tractography has at least three potential advantages.

First, it has the capability to elucidate branching pathways naturally like the fast-marching approach, which is an advantage compared to the streamline type methods. It is impossible for the existing streamline-based tracking methods to generate diverging fiber trajectories when the tracing starts from a single point [54]. When multiple fiber bundles are generated by using these schemes with the same region of interest, the density of trajectories will be reduced and the subsequent connected regions are undersampled. There is no such undersampling problem for the branching process in the DFTA since the algorithm follows all branching pathways in the same manner, computing diffusion fronts consecutively. The fast marching tractography developed in [53,54] also presents the desired feature to allow tract branching, in which the fast marching technique is adopted in the context of the diffusion tensor field to propagate fronts that evolve at a rate controlled by the information contained in the principal eigenvector field. Compared to the fast marching approach, DFTA relies on direct simulation of the diffusion process to construct successive diffusion fronts, and more importantly, the diffusion simulation is more problem-oriented than the level set-based methods which are more general purpose oriented.

The second feature of the diffusion simulation-based method is that it is likely to enhance the robustness and reliability in fiber reconstruction. DFTA has a lower chance to get affected by the noise since more information from the diffusion simulation is involved in determining the fiber pathways, helping partially restrain the noise problem, although it does use the principal eigenvector to regulate the path curvature.

The third feature of DFTA is its generality in its formulation. The governing equation (8) can accommodate generalized diffusion formulation for more advanced imaging modalities, such as the high angular diffusion weighted imaging (HARDI) [68] and the generalized diffusion tensors [41]. Because DFTA simulates the underlying physical diffusion process, which is what the

diffusion-weighted imaging measures, it is virtually independent of the particular imaging modality used to acquire the images.

Further investigation and demonstrations are needed to determine if it is possible for DFTA to get through regions with low anisotropy to find fiber pathways, and thus to avoid dropouts (premature interrupts) of fiber tracking, and to partly overcome the partial volume effects. Although this class of techniques has this potential, it is difficult to validate the accuracy of the crossing fibers and rule out the possibility of false fiber courses. Another limitation of this method is that the spatial resolution of the measured diffusion tensor data likely affects its ability to track small fiber tracts and the fiber bundles with high curvatures, such as those in the reconstruction of the optic radiation.

7. Applications

DT-MRI fiber tractography provides unique quantitative and qualitative information to aid in visualizing and in *in vivo* studying fiber tract architecture inside the human brain. This field of research is still in its infancy but is developing very fast. There exist many possible and important applications for the fiber tractography, and more will appear in the future as DT-MRI and fiber tracking become standard clinical procedures. A few potentially important applications are:

- Brain surgery, which may cause damage to important fiber bundles. Knowledge of their extension can be used to avoid damage to the major fiber tracts and to minimize the functional damage to the patients [71].
- White matter could be visualized using fiber tractography for a better understanding of the brain anatomy. The tractography can be used for segmentation of white matter tissues [24,80]. Successive DT-MRI measurements at different ages can be used to monitor the development of human brains [40,72] and the possible development of certain brain disorders.
- Connectivity between different parts of the brain could be inferred, which is useful for functional and morphological research on the brain [43]. This is a very promising potential research topic for the combination of DT-MRI and fMRI [21].
- Clinical applications to study the degeneration of white matter tissues and the disruption of fiber pathways due to different brain disorders [32,59,64].

To date, most clinical applications of DT-MRI are limited to the comparison of FA values or other anisotropy measures in some regions of interests of the brain [12,58,77,78]. It would be more interesting and more informative to visualize the disruption of the fiber pathways due to the disease progression, which can be done by using fiber tractography. For instance, Fig. 5 shows the reconstructed fiber tracts of the genu of the corpus callosum of a healthy person and an age-matched early Alzheimer's disease patient. It can be seen clearly that the full genu tract of the healthy person can be reconstructed, but the genu tract of the early Alzheimer's disease patient is

obviously disrupted and disconnected. By monitoring the integrity of certain fiber tracts, it may be possible to monitor the progress of this disease and to provide early warnings for possible interventions.

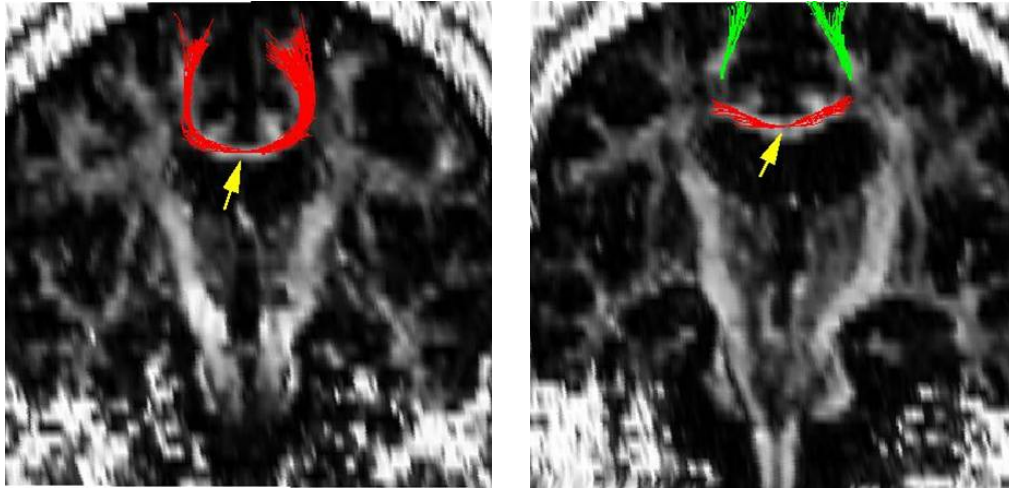


Figure 5: Reconstructed tracts of the genu of the corpus callosum of a healthy person (left) and an age-matched early Alzheimer's disease patient (right).

Also, DT-MRI fiber tractography could be applied to other fibrous tissues besides the human brain, such as the heart, whose fiber directional pattern and organization is critical in following its normal development and diagnosing diseases.

8. Fiber Tractography and Visualization Software Packages

The following are some of the available fiber tractography and visualization software packages:

- 3DMRI
3DMRI is developed at the Laboratory of Brain Anatomical Imaging, Johns Hopkins Medical Institute, Johns Hopkins University. It is a C++ application built on top of the Visualization Toolkit (VTK) to visualize fiber tracts. Fiber tracts are visualized inside an isosurface of human brain generated from brain MRI scan. Users can change the transparency of the isosurface and can assign colors and thickness to fiber tracks. Also, users can choose to project the fibers to the brain cortex to estimate possible contact area. This software is available at:
<http://cmrm.med.jhmi.edu/DTIuser/DTIuser.asp>
- 3D Slicer
3D Slicer is a software tool for guiding biopsies and craniotomies in the operating room,

offering diagnostic visualization and surgical planning in the clinic, and facilitating research into brain shift and volumetric studies in the lab. It provides capabilities for automatic registration (aligning data sets), semi-automatic segmentation (extracting structures such as vessels and tumors from the data), generation of 3D surface models (for viewing the segmented structures), 3D visualization, and quantitative analysis (measuring distances, angles, surface areas, and volumes) of various medical scans. 3D slicer is developed by collaboration between the MIT Artificial Intelligence Lab and the Surgical Planning Lab at Brigham & Women's Hospital, an affiliate of Harvard Medical School. Windows, Solaris and Linux versions of the 3D Slicer are all provided. The download information is available at:

<http://www.slicer.org>

- DTIChecker

DTIChecker is a tool, written by P. Fillard², to generate fiber tracts from diffusion tensor images. The latest stable release version is 1.2, which supports Windows, Linux and Solaris. The original tracking algorithm and first C++ code were developed by Xu *et al.* [76]. The download information is available at:

<http://www.ia.unc.edu/dev/download/fibertracking/index.htm>

- DdDTI

DoDTI is a software toolkit developed for the analysis and quantification of diffusion tensor imaging, which includes techniques for visualization and fiber tractography on DT-MRI data. It is a platform independent tool implemented in Matlab. The tracking algorithm embedded is based on the streamline tracking technique using a 4th order Runge-Kutta integration solver. The current version of DoDTI is v.1.0. More information about the toolkit, including its download information can be accessed at:

<http://neuroimage.yonsei.ac.kr/dodti>.

- dTV

The diffusion tensor visualizer (dTV) is an extension program developed for the volume data view program VOLUME-ONE.³ dTV performs analysis of DT-MRI data and transfers results to VOLUME-ONE for display. It is developed by Y. Masutani.⁴ The download link is:

http://www.ut-radiology.umin.jp/people/masutani/dTV/dTV_download-e.htm

9. Beyond DT-MRI

Tissues with regularly ordered microstructure, such as skeletal muscle, spine, tongue, heart, cerebral white matter, exhibits anisotropic water diffusion due to the alignment of the diffusion compartments in the tissue. The direction of the preferred diffusion and the implied direction of the tissue orientation can be obtained *in vivo* by DT-MRI. DT-MRI measures the apparent water

² pierre.fillard@wanadoo.fr, Department of Computer Science, University of North Carolina, Chapel Hill, USA

³ VOLUME-ONE is a free software for viewing volumetric image data such as X-ray CT and MRI. More information can be found at: <http://www.volume-one.org>

⁴ Department of Radiology, University of Tokyo Hospital, <http://www.ut-radiology.umin.jp/people/masutani/>

self-diffusion tensor under the assumption of Gaussian diffusion. This assumption makes the tensor model incapable of resolving *multiple fiber orientations within an individual voxel* in the streamline-based fiber tracking algorithms [2]. However, DFTA can alleviate the fiber crossing problem, as we demonstrated in the previous section.

At the millimeter-scale resolution typical of DT-MRI, the volume of cerebral white matter may contain several fibers running along the same directions, given the widespread divergence and convergence of fascicles. Such phenomenon is called *intervoxel orientational heterogeneity* (IVOH) [68]. This shortcoming of DT-MRI motivates researchers to consider alternative imaging techniques to resolve IVOH, such as fiber crossing. New diffusion-weighted imaging techniques, such as the high angular resolution diffusion imaging (HARDI) [19,69,70], q-space imaging (QSI) [68], or generalized diffusion tensor imaging (GDTI) [41], etc. These imaging techniques make use of a large number of diffusion-weighted images taking along different angular directions. They hold the promise of distinguishing more complex fiber structures than DT-MRI, with the drawback of much longer imaging acquisition time and lower signal-to-noise ratios. Moreover, fiber tractography based on these new imaging techniques are still under development.

An outstanding feature of the fiber reconstruction technique using diffusion simulations is that it can be seamlessly adapted to the platform established by the new imaging techniques. Studies have shown that the generalized diffusion tensor model is able to not only accommodate HARDI and GDTI methods but QSI as well, due to the relationships among DT-MRI, HARDI, GDTI, and QSI [41,49]. This makes it possible for the diffusion simulation based tractography to become independent of the imaging techniques used, while the fiber tracking will require a more sophisticated diffusion simulation, which is governed by a generalized diffusion equation associated with generalized diffusion tensors, according to a generalization of Fick's second law.

References

- [1] A. L. Alexander, K. M. Hasan, L. Mariana, J. S. Tsuruda, and D. L. Parker. Analysis of partial volume effects in diffusion-tensor MRI. *Magn. Reson. Med.*, 45:770-780, 2001.
- [2] D. C. Alexander, G. J. Barker and S. R. Arridge. Detection and modelling of non-Gaussian apparent diffusion coefficient profiles in human brain data. *Magn. Reson. Mde.* 48:331-340, 2002.
- [3] B. A. Ardekani, J. Nierenberg, M. J. Hoptman, D. C. Javitt, and K. O. Lim. MRI study of white matter diffusion anisotropy in schizophrenia. *Neuroreport*, 14(16):2025-2029, 2003.
- [4] P. J. Basser and D. K. Jones. Diffusion-tensor MRI: theory, experimental design and data analysis - a technical review. *NMR Biomed.*, 15:456-467, 2002.
- [5] P. J. Basser, J. Mattiello, and D. Le Bihan. Estimation of the effective self-diffusion tensor from the NMR spin echo. *J. Magn. Reson., Ser. B*, 103:247-254, 1994.
- [6] P. J. Basser, S. Pajevic, C. Pierpaoli, J. Duda, and A. Aldroubi. In vivo fiber tractography

- using DT-MRI data. *Magn. Reson. Med.*, 44:625-632, 2000.
- [7] P. J. Basser and C. Pierpaoli. Microstructural and physiological features of tissues elucidated by quantitative-diffusion-tensor MRI. *J. Magn. Reson. Med., Ser. B*, 111:209-219, 1996.
- [8] P. G. Batchelor, D. L. G. Hill, D. Atkinson, F. Calamante, and A. Connelly. Fiber-tracking by using diffusion-convection equation. *ISMRM*. 2002.
- [9] P. G. Batchelor, D. L. G. Hill, F. Calamante, and D. Atkinson. Study of connectivity in the brain using the full diffusion tensor from MRI. In *Information Processing in Medical Imaging, Proceedings of the 17th International Conference, IPMI'01*, pages 121-133. Springer-Verlag, New York, NY, 2001.
- [10] C. Beaulieu. The basis of anisotropic water diffusion in the nervous system – a technical review. *NMR Biomed.*, 15:435-455, 2002.
- [11] A. B. M. Bjornemo. *White Matter Fiber Tracking Using Diffusion Tensor MRI*. M.S. Thesis, Linköping University, Sweden, 2002.
- [12] M. Bozzali, A. Falini, M. Franceschi, M. Cercignani, M. Zuffi, G. Scotti, G. Comi, and M. Filippi. White matter damage in Alzheimer's disease assessed in vivo using diffusion tensor magnetic resonance imaging. *J. Neurol. Neurosurg. Psychiatry*, 72:742-746, 2002.
- [13] H. S. W. Campbell, K. Siddiqi, B. C. Vemuri, and G. B. Pike. A geometric flow for white matter fiber tract reconstruction. In *Proceedings of IEEE Int. Symposium on Biomedical Imaging Conference*, pages 505-508, 2002.
- [14] T. E. Conturo, N. F. Lori, T. S. Cull, E. Akbudak, A. Z. Snyder, J. S. Shimony, R. C. McKinstry, H. Burton, and M. E. Raichle. Tracking neuronal fiber pathways in the living human brain. *Proc. Natl. Acad. Sci. USA*, 96:10422-10427, 1999.
- [15] A. F. M. DaSilva, D. S. Tuch, M. R. Wiegell, and N. Hadjikhani. A primer on diffusion tensor imaging of anatomical substructures. *Neurosurg. Focus*, 15(1):1-4, 2003.
- [16] A. Fick. Über diffusion. *Ann. Phys.*, pages 94-99, 1855.
- [17] M. Filippi, M. Cercignani, M. Inglese, M. A. Horsfield, and G. Comi. Diffusion tensor magnetic resonance imaging in multiple sclerosis. *Neurology*, 56:304-311, 2001.
- [18] J. Foong, M. Maier, C. A. Clark, G. J. Barker, D. H. Miller, and M. A. Ron. Neuropathological abnormalities of the corpus callosum in schizophrenia: a diffusion tensor imaging study. *J. Neuroal Neurisurg. Psychiatry*, 68(2):242-244, 2000.
- [19] L. R. Frank. Characterization of anisotropy in high angular resolution diffusion-weighted MRI.

- Magn. Reson. Med.*, 47:1083-1099, 2002.
- [20]D. Gembris, H. Schumacher, and D. Suter. Solving the diffusion equation for fiber tracking in the living human brain. In *Proceedings of the International Society for Magnetic Resonance Medicine (ISMRM)*, volume 9, page 1529, Glasgow, Scotland, July 1999.
- [21]M. Guye, G. J. M. Parker, M. Symms, P. Boulby, C. A. M. Wheeler-Kingshott, A. Salek-Haddadi, G. J. Baker, and J. S. Duncan. Combined functional MRI and tractography to determine the connectivity of the human primary motor cortex in vivo. *NeuroImage*, 19:1349-1360, 2003.
- [22]S. Heim, K. Hahn, P. G. Sämann, L. Fahrmeir, and D. P. Auer. Assessing DTI data quality using bootstrap analysis. *Magn. Reson. Med.*, 52:582-589, 2004.
- [23]H. Huang, J. Zhang, P. C. M. van Zijl, and S. Mori. Analysis of noise effects on DTI-based tractography using the brute-force and multi-ROI approach. *Magn. Reson. Med.*, 52:559-565, 2004.
- [24]L. Jonasson, X. Bresson, P. Hagmann, O. Cuisenaire, R. Meuli, and J.-P. Thiran. White matter fiber tract segmentation in DT-MRI using geometric flows. *Medical Image Anal.*, 2005. to appear.
- [25]L. Jonasson, P. Hagmann, X. Bresson, R. Meuli, O. Cuisenaire, and J.-P. Thiran. White matter mapping in DT-MRI using geometric flows. In *Proceedings of the 9th International Workshop on Computer Aided Systems Theory*, volume LNCS 2809, pages 585-596, Las Palmas de Gran Canaria, Spain, 2003.
- [26]D. K. Jones, D. Lythgoe, M. A. Horsfield, A. Simmons, S. C. Williams, and H. S. Markus. Characterization of white matter damage in ischemic leukoaraiosis with diffusion tensor MRI. *Stroke*, 30:393-397, 1999.
- [27]N. Kang, J. Zhang, and E. S. Carlson. Parallel simulation of anisotropic diffusion with human brain DT-MRI data. *Computers and Structures*, 82:2389-2399, 2004.
- [28]N. Kang, J. Zhang, and E. S. Carlson. Performance of ILU preconditioning techniques in simulating anisotropic diffusion in the human brain. *Future Generation Comput. System*, 20:687-698, 2004.
- [29]N. Kang, J. Zhang, and E. S. Carlson. Tracking white matter fiber in human brain. *Journal of Shanghai University*, 10 (suppl.):13-17, 2004.
- [30]N. Kang, J. Zhang, and E. S. Carlson. Fiber tracking by simulating diffusion process with diffusion kernels in the human brain with DT-MRI data. Technical Report No. 428-05, Department of Computer Science, University of Kentucky, Lexington, KY, 2005.

- [31]N. Kang, J. Zhang, E. S. Carlson, and Daniel Gembris. White matter fiber tractography via anisotropic diffusion simulation in the human brain. Technical Report No. 410-04, Department of Computer Science, University of Kentucky, Lexington, KY, 2004.
- [32]S. M. Kealey, Y.-J. Kim, and J. M. Provenzale. Redefinition of multiple sclerosis plaque size using diffusion tensor MRI. *AJR*, 183:497-503, 2004.
- [33]M A. Koch, D. G. Norris, and M. Hund-Georgiadis. An investigation of functional and anatomical connectivity using magnetic resonance imaging. *NeuroImage*, 16:241-250, 2002.
- [34]M. Kubicki, C.-F. Westin, S. E. Maier, H. Mamata, M. Frumin, H. Erner-Hershfield, R. Kikinis, F. A. Jolesz, R. McCarley, and M. E. Shenton. Diffusion tensor imaging and its application to neuropsychiatric disorders. *Harvard Rev. Psychiatry*, 10:324-336, 2002.
- [35]L. L. Latour, K. Svoboda, P. P. Mitra, and C. H. Sotak. Time-dependent diffusion of water in a biological model system. *Proc. Natl. Acad. Sci. USA*, 91:1229-1233, 1994.
- [36]M. Lazar, D. M. Weinstein, J. S. Tsuruda, K. M. Hasan, K. Arfanakis, M. E. Meyerand, B. Badie, H. A. Rowley, V. Haughton, A. Field, and L. A. Alexander. White matter tractography using diffusion tensor deflection. *Human Brain Mapping*, 18:306-321, 2003.
- [37]D. Le Bihan, E. Breton, D. Lallemand, P. Grenier, E. A. Cabanis, and M. Laval-Jeantet. MR imaging of intravoxel incoherent motions: application to diffusion and perfusion in neurological disorders. *Radiology*, 161:401-407, 1986.
- [38]D. Le Bihan, J. F. Mangin, C. Poupon, C. A. Clark, S. Pappata, N. Molko, and H. Chabriat. Diffusion tensor imaging: concepts and application. *J. Magnetic Resonance Imaging*, 31:534-546, 2001.
- [39]D. Le Bihan and P. van Zijl. From the diffusion coefficient to the diffusion tensor. *NMR Biomed.*, 15:431-434, 2002.
- [40]T.-Q. Li and M. D. Noseworthy. Mapping the development of white matter tracts with diffusion tensor imaging. *Developmental Science*, 5(3):293-300, 2002.
- [41]C. Liu, R. Bammer, B. Acar, and M. E. Moseley. Characterizing non-Gaussian diffusion by using generalized diffusion tensors. *Magn. Reson. Med.*, 51:924-937, 2004.
- [42]N. F. Lori, E. Akbudak, J. S. Shimony, T. S. Cull, A. Z. Snyder, R. K. Guillory, and T. E. Conturo. Diffusion tensor fiber tracking of human brain connectivity: acquisition methods, reliability analysis and biological results. *NMR Biomed.*, 15:493-515, 2002.
- [43]J.-F. Mangin, C. Poupon, Y. Cointepas, D. Rivière, D. Papadopoulos-Orfanos, C. A. Clark,

- and J. Régis. A framework based on spin glass models for the inference of anatomical connectivity from diffusion-weighted MR data - a technical review. *NMR Biomed.*, 15:481-492, 2002.
- [44]S. Mori, B. J. Crain, V. P. Chacko, and P. C. M. van Zijl. Three-dimensional tracking of axonal projections in the brain by magnetic resonance imaging. *Ann. Neurol.*, 45:265-269, 1999.
- [45]S. Mori and P. C. M. van Zijl. Fiber tracking: principles and strategies - a technical review. *NMR Biomed.*, 15:468-480, 2002.
- [46]M. Moseley. Diffusion tensor imaging and aging - a review. *NMR Biomed.*, 15:553-560, 2002.
- [47]C. Nicholson. Diffusion and related transport mechanism in brain tissue. *Reports on Progress in Physics*, 64:815-884, 2001.
- [48]L. O'Donnell, S. Haker, and C.-F. Westin. New approaches to estimation of white matter connectivity in diffusion tensor MRI: elliptic PDEs and geodesics in a tensor-warped space. In *Proceedings of the Fifth Int. Conf. on Medical Image Computing and Computer-Assisted Intervention (MICCAI'2002), Part I*, page 564-571, Tokyo, Japan, September 25-28 2002.
- [49]E. Özarslan and T. H. Mareci. Generalized diffusion tensor imaging and analytical relationships between diffusion tensor imaging and high angular resolution diffusion imaging. *Magn. Reson. Med.*, 50:955-965, 2003.
- [50]S. Pajevic, A. Aldroubi, and P. J. Basser. A continuous tensor field approximation of discrete DT-MRI data for extracting microstructural and architectural features of tissue. *J. Magnet. Reson.*, 154:85-100, 2002.
- [51]G. J. M. Parker and D. C. Alexander. Probabilistic Monte Carlo based mapping of cerebral connections utilising whole-brain crossing fibre information. In C. J. Taylor and A. Noble, editors, *Information Processing in Medical Imaging (IPMI'03)*, volume LNCS 2737, pages 684-695, 2003.
- [52]G. J. M. Parker, H. A. Haroon, and C. A. M. Wheeler-Kingshott. A framework for a streamline-based probabilistic index of connectivity (PICO) using a structural interpretation of MRI diffusion measurements. *J. Magn. Reson. Imaging*, 18:242-254, 2003.
- [53]G. J. M. Parker, K. E. Stephan, G. J. Barker, J. B. Rowe, D. G. MacManus, C. A. M. Wheeler-Kingshott, O. Ciccarelli, R. E. Passingham, R. L. Spinks, R. N. Lemon, and R. Turner. Initial demonstration of in vivo tracing of axonal projections in the macaque brain and comparison with the human brain using diffusion tensor imaging and fast marching tractography. *NeuroImage*, 15:797-809, 2002.
- [54]G. J. M. Parker, C. A. M. Wheeler-Kingshott, and G. J. Barker. Estimating distributed

- anatomical connectivity using fast marching methods and diffusion tensor imaging. *IEEE Transactions on Medical Imaging*, 21(5):505-512, 2002.
- [55] A. Pfefferbaum and E. V. Sullivan. Increased brain white matter diffusivity in normal adult aging: relationship to anisotropy and partial voluming. *Magn. Reson. Med.*, 49:953-961, 2003.
- [56] A. Pfefferbaum, E. V. Sullivan, M. Hedehus, and et al. Age related decline in brain white matter anisotropy measured by spatially corrected echo-planar diffusion tensor imaging. *Magn. Reson. Med.*, 44:259-268, 2000.
- [57] C. Poupon, J. F. Mangin, C. A. Clark, V. Frouin, J. Régis, D. Le Bihan, and I. Bloch. Towards inference of human brain connectivity from MR diffusion tensor data. *Medical Image Anal.*, 5:1-15, 2001.
- [58] S. E. Rose, F. Chen, J. B. Chalk, F. O. Zelaya, W. E. Strugnell, M. Benson, and et al. Loss of connectivity in Alzheimer's disease: an evaluation of white matter tract integrity with colour coded MR diffusion tensor imaging. *J. Neurol. Neurosurg. Psychiatry*, 69:528-530, 2000.
- [59] M. Sach, G. Winkler, V. Glauche, J. Liepert, B. Heimbach, M. A. Koch, C. Büchel, and C. Weiller. Diffusion tensor MRI of early upper motor neuron involvement in amyotrophic lateral sclerosis. *Brain*, 127:340-350, 2004.
- [60] J. A. Sethian. A fast marching level set method for monotonically advancing fronts. *Proc. Natl. Acad. Sci. USA*, 93:1591-1595, 1996.
- [61] J. A. Sethian. *Level Set Methods and Fast Marching Methods*. Cambridge Press, Cambridge, MA, 2 edition, 1999.
- [62] B. Stieltjes, W. E. Kaufmann, P. C. M. van Zijl, K. Fredericksen, G. D. Pearlson, M. Solaiyappan, and S. Mori. Diffusion tensor imaging and axonal tracking in the human brainstem. *NeuroImage*, 14:723-735, 2001.
- [63] B. Stieltjes, M. Schluter, H. K. Hahn, T. Wilhelm, and M. Essig. Diffusion tensor imaging: theory, sequence optimization and application in Alzheimer's disease. *Radiology*, 43(7):562-565, 2003.
- [64] P. C. Sundgren, Q. Dong, D. Gómez-Hassan, S. K. Mukherji, P. Maly, and R. Welsh. Diffusion tensor imaging of the brain: review of clinical applications. *Neuroradiology*, 46:339-350, 2004.
- [65] C. R. Tench, P. S. Morgan, L. D. Blumhardt, and C. Constantinescu. Improved white matter fiber tracking using stochastic labeling. *Magn. Reson. Med.*, 48:677-683, 2002.
- [66] A. L. Tievsky, T. Park, and J. Farkas. Investigation of apparent diffusion coefficient and

- diffusion tensor anisotropy in acute and chronic multiple sclerosis lesions. *Am. J. Neuroradiol.*, 20:1491-1499, 1999.
- [67]J. D. Tournier, F. Calamante, D. G. Gadian, and A. Connelly. Diffusion-weighted magnetic resonance imaging fibre tracking using a front evolution algorithm. *NeuroImage*, 20:276-288, 2003.
- [68]D. S. Tuch. *Diffusion MRI of Complex Tissue Structure*. PhD thesis, Harvard University-Massachusetts Institute of Technology, Cambridge, MA, 2002.
- [69]D. S. Tuch, T. G. Reese, M. R. Wiegell, N. Makris, J. W. Belliveau, and V. J. Wedeen. High angular resolution diffusion imaging reveals intravoxel white matter fiber heterogeneity. *Magn. Reson. Med.*, 48:577-582, 2002.
- [70]D. S. Tuch, T. G. Reese, M. R. Wiegell, and V. J. Wedeen. Diffusion MRI of complex neural architecture. *Neuron*, 40:885-895, 2003.
- [71]S. K. Warfield, F. Talos, A. Tei, A. Bharatha, A. Nabavi, M. Ferrant, P. M. Black, F. A. Jolesz, and R. Kikinis. Real-time registration of volumetric brain MRI by biomechanical simulation of deformation during image guided neurosurgery. *Comput. Visual. Sci.*, 5:3-11, 2002.
- [72]R. Watts, C. Liston, S. Niogi, and A. M. Uluğ. Fiber tracking using magnetic resonance diffusion tensor imaging and its applications to human brain development. *MRDD Research Reviews*, 9:168-177, 2003.
- [73]D. Weinstein, G. Kindlmann, and E. Lundberg. Tensorlines: advection-diffusion based propagation through diffusion tensor fields. In *Proceedings of IEEE Visualization Conference*, pages 249-253, San Francisco, CA, 1999.
- [74]C.-F. Westin, S. E. Maier, H. Mamata, A. Nabavi, F. A. Jolesz, and R. Kikinis. Processing and visualization for diffusion tensor MRI. *Medical Image Analysis*, 6:93-108, 2002.
- [75]M. R. Wiegell, H. B. W. Larsson, and V. J. Wedeen. Fiber crossing in human brain depicted with diffusion tensor MR imaging. *Radiology*, 217:897-903, 2000.
- [76]D. Xu, S. Mori, M. Solaiyappan, P. C. M. van Zijl, and C. Davatzikos. A framework for callosal fiber distribution analysis. *NeuroImage*, 17:1131-1143, 2002.
- [77]T. Yoshiura, F. Mihara, K. Ogomori, A. Tanaka, K. Kaneko, and K. Masuda. Diffusion tensor in posterior cingulate gyrus: correlation with cognitive decline in Alzheimer's disease. *NeuroReport*, 13:2299-2302, 2002.
- [78]T. Yoshiura, F. Mihara, A. Tanaka, K. Ogomori, Y. Ohyagi, T. Taniwaki, T. Yamada, T. Yamasaki, A. Ichimiya, N. Kinukawa, Y. Kuwabara, and H. Honda. High b value

diffusion-weighted imaging is more sensitive to white matter degeneration in Alzheimer's disease. *NeuroImage*, 20:413-419, 2003.

[79]L. Zhukov and A. Barr. Oriented tensor reconstruction: tracking neural pathways from diffusion tensor MRI. In *Proceedings of the IEEE Visualization*, 2002.

[80]L. Zhukov, K. Museth, D. Breen, R. Whitaker, and A. Barr. Level set modeling and segmentation of DT-MRI brain data. *J. Electronic Imaging*, 12:125-133, 2003.